

Evidence of random spin-singlet state in a three-dimensional quantum spin liquid candidate $\text{Sr}_3\text{CuNb}_2\text{O}_9$

S. M. Hossain,¹ S. S. Rahaman,² H. Gujrati,¹ Dilip Bhoi,³ A. Matsuo,³ K. Kindo,³ M. Kumar,^{2,*} and M. Majumder^{1,†}

¹*Department of Physics, Shiv Nadar Institution of Eminence,
Gautam Buddha Nagar, Uttar Pradesh 201314, India*

²*S.N. Bose National Centre for Basic Sciences, Salt Lake, Kolkata 700106, India*

³*The Institute for Solid State Physics, University of Tokyo, Kashiwa, Chiba 277-8581, Japan.*

(Dated: July 1, 2024)

Disorder is ubiquitous in any quantum many-body system and is usually considered to be an obstacle to the elucidation of the underlying physics of complex systems, but its presence can often introduce exotic phases of matter that cannot generally be realized in a clean system. We report here a detailed experimental and theoretical study of magnetic properties of highly disordered $\text{Sr}_3\text{CuNb}_2\text{O}_9$ material which exhibits random site mixing between Cu and Nb. The magnetic moments (Cu^{2+}) are arranged in a quasi-cubic (three-dimensional) manner, leading to a high degree of frustration with a Curie-Weiss temperature (θ_{CW}) of about -60 K without any long-range magnetic ordering down to 466 mK. These observations suggest that $\text{Sr}_3\text{CuNb}_2\text{O}_9$ is a candidate for a quantum spin liquid. More interestingly, the susceptibility ($\chi = M/\mu_0 H$) and the C_m/T (C_m is the magnetic part of the heat capacity) follow a power-law behavior with decreasing temperature. In addition, $M(T, \mu_0 H)$ and $C_m(T, \mu_0 H)/T$ show scaling relationships over a wide temperature and field range. This unusual behavior with respect to the conventional behavior of a QSL can be discussed qualitatively as the coexistence of a disorder-induced random spin singlet (RSS) state and a QSL state. A quantitative description has been given by numerical calculations considering a power-law probability distribution $P(J) \propto J^{-\gamma}$ (J is the exchange interaction) of random spin singlets. The parameters extracted from the numerical calculations are in excellent agreement with the experimental data. Furthermore, the analytical results are also consistent with the power-law and scaling behavior of χ and $C_m(T, \mu_0 H)/T$ as a whole. Thus, our comprehensive experimental and theoretical analysis provides evidence for the stabilization of the RSS state in a three-dimensional lattice.

Introduction: The presence of disorder is inevitable in any real-life quantum many-body system and it hinders us from elucidating the actual physics of a system. More specifically, the effects of disorder on the phases or phase transitions in quantum many-body systems is reflected by the disappearance of spontaneous symmetry breaking or smearing out the singularities associated with phase transitions and critical phases [1]. On the contrary, there are also examples of exotic ground states and new phenomena driven by disorder, which can not be realized in a clean or disorder-free system. Thus, discovering and characterizing those ground states in a quantum many-body system where there exists the interplay of disorder and quantum fluctuations is a current field of study in condensed matter physics [1, 2]. These systems are also crucial for several application purposes, e.g. they can be the key elements for memories and state transfer channels in quantum computing [3–6]. One of the first prominent examples of disorder-driven states is Anderson localization, where the wavefunction of non-interacting quantum particles is highly localized near a point in space due to a strong random potential [7, 8]. Recently, disorder-driven topological Anderson localization has also been observed [9, 10]. Quasi-particle interference (QPI) is a powerful experimental tool and it originates because of the

presence of disorder and helps to explore the momentum space informations in a 2D system[11]. Disorder-driven phenomena are also often observed in correlated many-body systems, e.g. Kondo disorder state, quantum Griffiths phase, which shows exotic non-Fermi liquid behaviors [1, 12–14]. Experimentally and theoretically, it was also observed that the presence of a strong disorder can turn the first-order magnetic phase transition to a second-order phase transition near the quantum critical point, and thus disorder-induced quantum critical point can be obtained [2, 15].

The effects of disorder in frustrated magnets is nowadays a focus area. Frustration may lead to a huge accidental degeneracy of different spin configurations and the ground state is the superposition of the degenerate states, known as the quantum spin liquid (QSL) state. In the QSL state, due to the absence of spontaneous symmetry breaking, the spins are dynamic even at $T = 0$ K and one can expect exotic fractionalized excitations.[16–18]. The presence of disorder in a frustrated system gives rise to a glassy state, the spin glass (SG) state [19]. Super-lattice structure produced by site disorder may also give rise to a frustrated triangular lattice and further may lead to the observation of a QSL state[20]. Very recently, it has been pointed out by Kimchi *et al.* that in some disordered frustrated systems, peculiar features in heat capacity and magnetization can be qualitatively explained as the presence of a "random spin-singlet" (RSS) state admixed with QSL state [21]. The RSS state have been first

* manoranjan.kumar@bose.res.in

† mayukh.cu@gmail.com

discussed for doped semiconductors in which the antiferromagnetic exchange energies follow a power-law probability distribution due to the presence of disorder [22–24]. Further, this idea of RSS state has also been extended to two-dimensional (2D) and three-dimensions (3D) [25–28] for doped semiconductors. Whereas, only a handful of the 2D frustrated systems show such exotic states where RSS state and QSL coexist [29–32] and so far the presence of such a state has not been observed in any 3D frustrated system experimentally. Note that in some 3D pyrochlore systems, the signature of QSL-like state was interpreted to be due to a RSS state but the probability distribution of exchange energies was not a power-law probability distribution [33]. Thus, discovering new three-dimensional systems with strong frustration along with disorder and elucidating the complex ground state qualitatively and quantitatively is a primary goal in this field. Needless to say that stabilizing such a state in a 3D lattice is inherently more challenging compared to low-dimensional systems, primarily due to the enhanced dimensionality reduces quantum fluctuations and hence more tendency to order magnetically.

In this letter, we have reported a detailed study of a three-dimensional quasi-cubic system $\text{Sr}_3\text{CuNb}_2\text{O}_9$. Magnetization and heat capacity measurements down to 466 mK indicate the absence of long-range magnetic ordering (LRO) despite a strong exchange interactions (of the order of -60 K) between Cu^{2+} -moments and thus established $\text{Sr}_3\text{CuNb}_2\text{O}_9$ as a 3D QSL candidate. Furthermore, the power-law divergence of susceptibility and heat capacity, along with the scaling behaviors of magnetization and heat capacity, indicate the presence of RSS state admixed with QSL due to the presence of strong Cu/Nb site disorder. Furthermore, numerical and analytical calculations described the experimental data quantitatively.

Crystal structure: Here $\text{Sr}_3\text{CuNb}_2\text{O}_9$ has been synthesized via a conventional solid-state reaction technique (details have been discussed in the supplementary materials[34]). $\text{Sr}_3\text{CuNb}_2\text{O}_9$ belongs to a family of triple perovskite crystal structures with a general formula $\text{A}_3\text{B}_3\text{O}_9$ shown in Fig.1(a). The compound stabilises in a tetragonal crystal structure of space group $P4/mmm$ (space group no. 123), with lattice parameters ($a = b \approx 3.953 \text{ \AA}$), $c = 4.089 \text{ \AA}$, and $\alpha = \beta = \gamma = 90^\circ$ obtained from PXRD rietveld refinement Fig.1(c). No extra peaks represent the existence of single-phase formation. Most importantly, no super lattice peaks have been detected, indicating a random distribution of Cu and Nb in contrast to $\text{Sr}_3\text{CuSb}_2\text{O}_9$ [20]. Thus, the magnetic skeleton is formed by Cu atoms randomly distributed over Nb sites, with occupancy ratios of 1/3 and 2/3, respectively and the in-plane distance between magnetic ions $\approx 3.95 \text{ \AA}$, whereas out-of-plane distance is $\approx 4.07 \text{ \AA}$, makes it almost a cubic magnetic lattice structure shown in Fig.1(b). Such a quasi-cubic 3D structure, if one considers the next nearest-neighbour interactions along with nearest-neighbour, may give rise to a 3D frustrated lattice. Thus, the present compound on the one hand, may

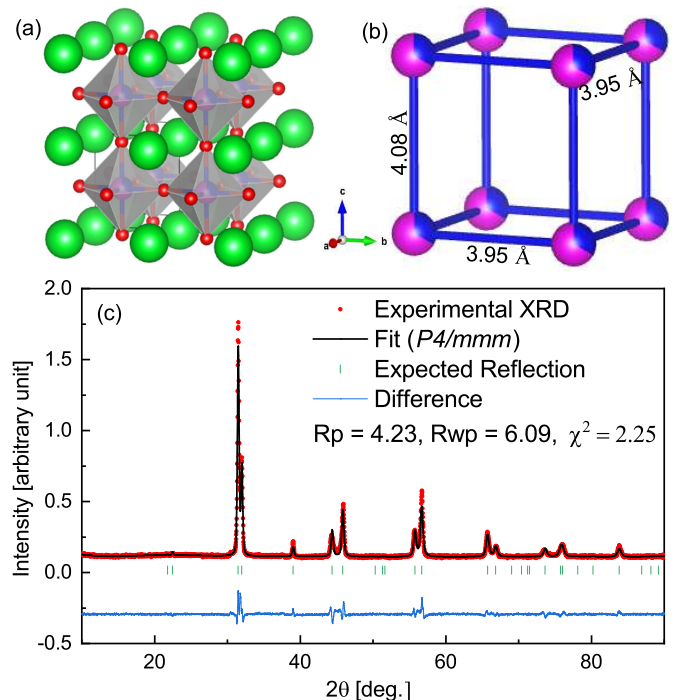


FIG. 1. (a) Magnetic sites forming an octahedral environment with the oxygen atoms (red) and the green spheres showing strontium atoms intercalated in between. (b) Arrangement of the magnetic Cu^{2+} (blue) sharing the same site with the non-magnetic Nb^{5+} (magenta). (c) A clean XRD pattern shows the absence of any impurity and has been analysed with the Rietveld refinement method.

provide a 3D frustrated lattice and, on the other hand, provide strong disorder (random site-disorder of Cu and Nb), which may then be favourable to realize a RSS state. In order to verify our expectation from the structural analysis, we have explored the ground state by performing detailed magnetization and heat capacity measurements in a broad temperature-field region.

Magnetization: Magnetic susceptibility ($\chi = M/\mu_0 H$) has been measured as a function of temperature at different applied magnetic fields. No anomaly associated with long-range magnetic ordering (LRO) has been observed down to 1.85 K as seen from Fig.2(a). The susceptibility data between 100-300 K, measurement at an applied magnetic field of 1 T, has been fitted with Curie-Weiss law ($\chi = \frac{C}{T - \theta_{CW}} + \chi_0$) shown as a solid line in Fig.2(a). Curie-Weiss temperature (θ_{CW}) obtained $\approx -60 \text{ K}$ with a curie constant $C = 0.49 \text{ cm}^3\text{Kmol}^{-1}$. The negative sign indicates the nature of exchanges is antiferromagnetic with a high degree of frustration parameter, defined as $f = \theta_{CW}/T_N$. For any magnetic system, θ_{CW} indicates the strength of exchange interactions between magnetic moments, and T_N is the ordering temperature. In the present systems, even though the moments are highly correlated with high θ_{CW} , the system cannot go to an LRO state at least down to 1.85 K due to strong

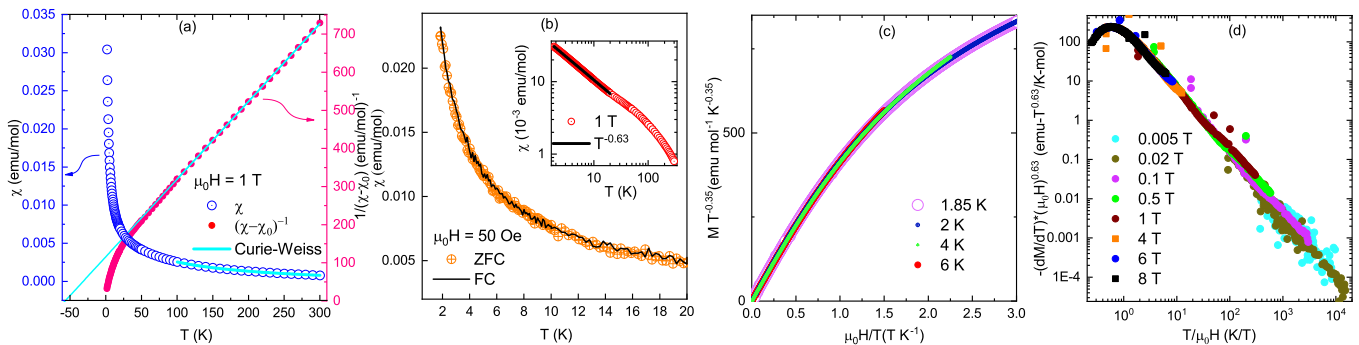


FIG. 2. (a) χ versus temperature at an applied magnetic field of 1 T (ZFC) and extrapolation of the Curie-Weiss fit (ranging from 100-300 K) in the inverse susceptibility data. (b) ZFC and FC data at 50 Oe applied magnetic field, and the inset shows the power-law behavior with the exponent $\gamma = 0.63$. (c) Scaling behavior of the magnetization data with respect to field at different temperatures with an exponent of $\gamma - 1 = 0.35$. (d) Scaling of the magnetization with respect to the temperature is showing excellent data collapse in a wide applied magnetic field range from 50 Oe to 8 T.

frustration. The effective moment has been calculated using the formula $\mu_{eff} = \sqrt{8C}$ gives $1.98 \mu_B$, where C is the Curie constant obtained from $1/\chi$ vs T fitting shown in Fig. 2(a). This indicates that the magnetic ions are in Cu^{2+} ($S=1/2$) state. Furthermore, the absence of branching in χ between the zero-field cooling and field cooling measured at 50 Oe rules out the possibility of spin freezing state (e.g. spin glass) at least down to 1.85 K (Fig. 2(b)). Thus, magnetization measurements ensure that $\text{Sr}_3\text{CuNb}_2\text{O}_9$ can be considered as a highly frustrated magnetic system promising to have a QSL ground state.

More interestingly, if one closely observes the temperature dependence of χ , then one can see that χ follows a power-law behavior ($T^{-\gamma}$) between 20 K to 1.85 K with γ to be 0.63. Such a power-law behavior was predicted to be a signature of RSS state in a frustrated system[21]. Along with the power-law in χ , the M versus $\mu_0 H$ data at different temperatures also collapses in one curve following a scaling behavior as shown in Fig.2(c) as $MT^{\gamma-1}$ against $\mu_0 H/T$. Even a scaling has also been observed in $(dM/dT) \times (\mu_0 H)^\gamma$ versus $T/\mu_0 H$. All these power-law and scaling behaviors support the presence of the predicted RSS state admixed with a QSL state.

Heat capacity: Heat capacity ($C_p(T, \mu_0 H)$) measurements have been performed from 300 K down to 466 mK at various applied magnetic fields to explore the ground state of $\text{Sr}_3\text{CuNb}_2\text{O}_9$. Fig.3(a) shows C_p versus T at different applied magnetic fields. The absence of any lambda-like anomaly indicates that $\text{Sr}_3\text{CuNb}_2\text{O}_9$ is avoided of any LRO down to 466 mK even though there is a strong correlation between magnetic moments and thus established that $\text{Sr}_3\text{CuNb}_2\text{O}_9$ is a 3D QSL candidate with a high degree of frustration ($f = \theta_{CW}/T_{min} \simeq 120$, where T_{min} represents the lowest temperature heat capacity has been measured). In general, C_p/T follows either exponential behaviour or power-law (T^γ) for a gapped and gapless QSL, respectively[35, 36]. In contrast to this expectation, C_p/T follows a power-law behavior

of $T^{-\gamma}$ in the present system at zero applied magnetic field. To get an qualitative description of the C_p data, we modeled it by considering three contributions as

$$C_p(T, \mu_0 H) = C_{ph} + C_{Sch} + C_{power-law} \quad (1)$$

where $C_{power-law} = A_{power-law} T^{1-\gamma}$ [29]. The other two terms C_{ph} , C_{Sch} represent phonon and two-level Schottky contribution (representing the hump), respectively. At sufficiently low temperatures, the phonon contribution behaves as $C_{ph} = \beta_{ph} T^3$, where β_{ph} is the Debye coefficient. And

$$C_{Sch} = A_{Sch} R \left[\frac{\Delta(\mu_0 H)}{k_B T} \right]^2 \frac{e^{\left(\frac{\Delta(\mu_0 H)}{k_B T} \right)}}{\left[1 + e^{\left(\frac{\Delta(\mu_0 H)}{k_B T} \right)} \right]^2} \quad (2)$$

where $\frac{\Delta}{k_B}$ represents the energy gap.

$C_m(\mu_0 H = 0)/T$ at zero field has been plotted as a function of temperature in Fig.3(b), which was estimated by subtracting the phonon (C_{ph}) and Schottky contributions (due to 1.8% of weakly coupled impurities; for details see [34]) from the total C_p . $C_m(\mu_0 H = 0)/T$ shows a power-law divergence with an exponent $\gamma = 0.58$ with lowering temperature. Also, note that the exponent γ is in agreement with the obtained γ from magnetization measurements.

From the qualitative analysis of the C_p it is now clear the spins are correlated (as it is seen from high θ_{CW}) and may form random singlets by a power-law distribution of exchange interactions due to the presence of strong site-disorder. Because of the power-law distribution of the exchange interactions (responsible for forming singlets), the excitations are gapless overall, giving rise to the power-law behavior in magnetization or heat capacity and eventually the scaling behaviors. These correlated spins (which form the singlets) may also form resonating state due to the presence of strong frustration, which may give rise to a QSL behavior.

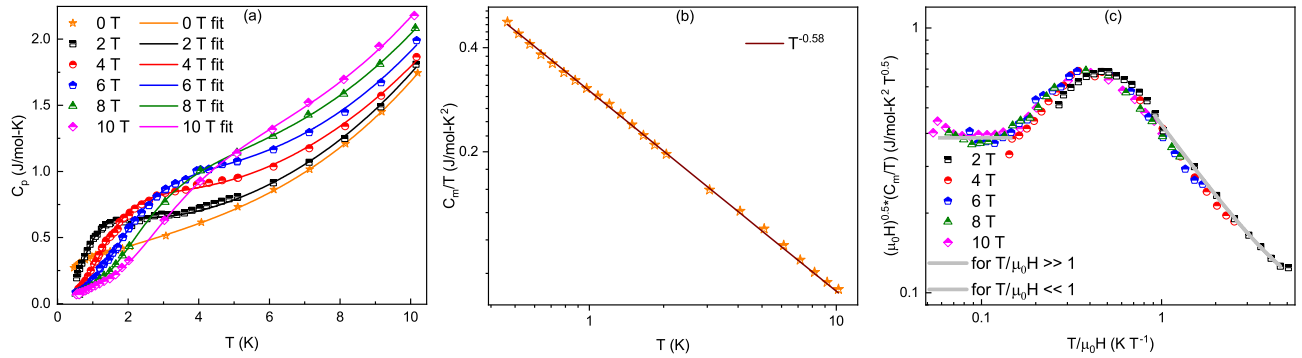


FIG. 3. (a) Temperature dependence of $C(T, \mu_0 H)$ at different applied magnetic fields. Solid lines show the fit considering three different contributions described in the text. (b) Power-law fit of the C_m/T (at 0 T) as a function of temperature with the an exponent of 0.58. (c) Scaling of the $C_m(T, \mu_0 H)/T$.

Kimchi *et al.*[21] pointed out that the magnetic contribution of the total heat capacity at finite fields (represented by $C_m(\mu_0 H) = C_p - C_{ph}$; see [34] for details) for this disorder-induced state, collapses into a single curve of the form

$$\frac{C_m[\mu_0 H, T]}{T} \sim \frac{1}{(\mu_0 H)^\gamma} F_q \left[\frac{T}{\mu_0 H} \right], \quad (3)$$

where $F_q(X)$ is a scaling function which is determined by the energy distribution of the singlets

$$F_q[X] \sim \begin{cases} X^q & X \ll 1 \\ X^{-\gamma} \left(1 + \frac{c_0}{X^2}\right) & X \gg 1 \end{cases} \quad (4)$$

where $q = 1$ and $q = 0$ represent the situation with and without Dzyaloshinskii-Moriya (DM) interactions in the effective low-energy theory coupling the orphan spins, respectively. Fig.3(b) represents $(\mu_0 H)^{0.5} \times C_m/T$ as a function of $T/\mu_0 H$ in which all the C_m data points fall on top of each other and thus validates the scaling relationship as proposed by the theory. In the range where $X \ll 1$, the data saturates, indicating the absence of DM interactions, whereas in the limit of $X \gg 1$, the data agrees reasonably well with the predicted scaling function Fig.3(c). It should be pointed out that, the scaling behavior still holds for the total heat capacity (see Fig.6 of the supplementary material[34]) except for the high-temperature region where the lattice contribution dominates.

Thus, the detailed magnetization and heat capacity measurements in a broad temperature and field range indicate a coexistence of RSS state and QSL state in a three-dimensional $\text{Sr}_3\text{CuNb}_2\text{O}_9$. Even though the experimental data represented here qualitatively matches the theoretical prediction, more quantitative description will be crucial to elucidate the underlying complex physics.

Theory: We further carried out numerical calculations to have a quantitative description of the temperature and field dependence of magnetization and heat capacity to confirm the possibility of the presence of RSS state in $\text{Sr}_3\text{CuNb}_2\text{O}_9$. To understand the magnetic properties of

the material we first analyze the percentage distribution ($\% \rho$) of Cu in various clusters of sizes up to $30 \times 30 \times 30$ cubic lattice of the compound $\text{Sr}_3\text{CuNb}_2\text{O}_9$ with only 33% of Cu. The distance between the two Cu atoms sitting in two nearest octahedra of the present compound is approximately 4 Å, therefore, a spin is a part of cluster if the distance of a spin is less than equal to 4 Å from any of spin in the cluster and with this criterion the percentage distribution ($\% \rho$) of the Cu atoms decays exponentially with cluster size (L) as shown in the supplementary material with the details of the calculation[34]. The most dominating spin clusters are free spins and part of these spins may be forming weakly interacting Cu structures with random exchange as the distances among the spins are larger than 4 Å and random. These spins can have comparable nearest, next-nearest exchanges due to their distribution in three-dimensional space. Therefore, these weakly interacting frustrated spins can be treated as random dimer singlet with a broad distribution of the exchanges. Other spin cluster bigger than dimer are very small in numbers and may have negligible effect on the magnetic properties of the material. Hence, we adopt an isotropic dimer Heisenberg spin-1/2 model Hamiltonian, incorporating a distribution of exchanges. This idea is inspired by the spin-1/2 model proposed by Dasgupta, Ma, and Fisher [22] for highly disordered one-dimensional systems, as well as the model presented by Bhatt and Lee [25] for highly disordered two and three-dimensional systems. The dimer model can be written as

$$H = \sum_i J_i S_{i,1} \cdot S_{i,2} = \sum_i H_i \quad (5)$$

where H_i is i^{th} isolated dimer Hamiltonian for spin 1 and 2, and J_i is isotropic exchange interaction of the i^{th} dimer. We assume J_i can take any continuous values (in between 0 and 1 in the reduced unit) and it follows the distribution $P(J) = J^{-\gamma}$, i.e. the smaller J has a higher probability distribution. A detailed description of the calculation is given in the Supplementary file[34].

We use $g = 2.22$, the average $J = \langle J_i \rangle \approx 72K$ and

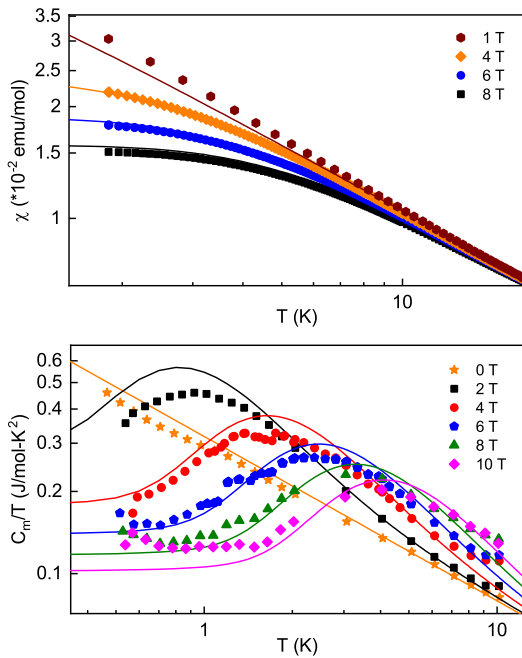


FIG. 4. Upper panel: Temperature dependence of χ (obtained experimentally) represented by the scattered points and the solid lines indicate the data obtained numerically. Lower panel: The solid lines and the scattered points represents experimentally and numerically obtained data of C_m/T .

$\gamma = 0.6$ to fit experimental curve of $C_m(T, \mu_0 H)/T$ and $\chi(T)$. The $\frac{M}{H}$ for four different fields are shown in the upper panel of Fig. 4, and $\chi (= \frac{M}{H})$ curves show a power-law decay as a function of temperature. The experimental curve of $C_m(T, \mu_0 H)/T$ is shown as points and the theoretical curve as lines for six different magnetic fields,

all the experimental curves can be fitted well with the theoretical curves as shown in lower panel of Fig. 4. In the lower panel of Fig. 4, the linear behavior of the C_m/T plot clearly shows the power-law behavior for the zero-field but finite field data shows criticality as a function of T and H . This behavior is well known as data-collapse in $\frac{T}{H}$ for the resonating limit $|J - H| < k_B T$. It is noticed that both $C_m(T, \mu_0 H)/T$ and χ can be fitted well with the experimental data with the same exponent which is 0.6 in this case. We analyse these results for different limits of temperature and field in the Supplementary file[34].

Thus, our numerical calculations quantitatively established that the temperature and field dependence of magnetization and heat capacity are due to the presence of disorder-driven RSS state.

Conclusion: The present manuscript has studied a novel disorder-induced state in great detail. We report here a comprehensive experimental and theoretical investigation of the compound $\text{Sr}_3\text{CuNb}_2\text{O}_9$. The disorder introduced by site-mixing between Cu and Nb and frustration due to competing nearest-neighbour and next nearest-neighbour of the three-dimensional quasi-cubic lattice gives rise to an exotic state in which RSS state coexists with QSL. Numerical calculations further gave a quantitative description of the experimental results and provided evidence of the realization of the RSS state in a three-dimensional lattice. Analytical calculations again confirm the experimentally observed behaviors of χ and $C_m(T, \mu_0 H)/T$. These observations established $\text{Sr}_3\text{CuNb}_2\text{O}_9$ as one of the rare compounds where such a RSS occurs in a 3D-lattice.

Acknowledgement: SMH and MM would like to acknowledge UGC-DAE Collaborative Research Scheme (ref. CRS/2021-22/01/393) for funding. MK thanks DST-SERB for funding through projects CRG/2020/000754.

-
- [1] T. Vojta, Disorder in quantum many-body systems, *Annual Review of Condensed Matter Physics* **10**, 233 (2019), <https://doi.org/10.1146/annurev-conmatphys-031218-013433>.
 - [2] A. G. Green, G. Conduit, and F. Krüger, Quantum order-by-disorder in strongly correlated metals, *Annual Review of Condensed Matter Physics* **9**, 59 (2018), <https://doi.org/10.1146/annurev-conmatphys-033117-053925>.
 - [3] R. Nandkishore and D. A. Huse, Many-body localization and thermalization in quantum statistical mechanics, *Annual Review of Condensed Matter Physics* **6**, 15 (2015), <https://doi.org/10.1146/annurev-conmatphys-031214-014726>.
 - [4] N. Y. Yao, L. Jiang, A. V. Gorshkov, Z.-X. Gong, A. Zhai, L.-M. Duan, and M. D. Lukin, Robust quantum state transfer in random unpolarized spin chains, *Phys. Rev. Lett.* **106**, 040505 (2011).
 - [5] J. Smith, A. Lee, P. Richerme, B. Neyenhuis, P. W. Hess, P. Hauke, M. Heyl, D. A. Huse, and C. Monroe, Many-body localization in a quantum simulator with programmable random disorder, *Nature Physics* **12**, 907 (2016).
 - [6] A. Kitaev, Anyons in an exactly solved model and beyond, *Annals of Physics* **321**, 2 (2006), january Special Issue.
 - [7] P. W. Anderson, Absence of diffusion in certain random lattices, *Phys. Rev.* **109**, 1492 (1958).
 - [8] A. Lagendijk, B. v. Tiggelen, and D. S. Wiersma, Fifty years of Anderson localization, *Physics Today* **62**, 24 (2009), <https://pubs.aip.org/physicstoday/article-pdf/62/8/24/11140320/24>
 - [9] Q. Lin, T. Li, L. Xiao, K. Wang, W. Yi, and P. Xue, Observation of non-hermitian topological anderson insulator in quantum dynamics, *Nature Communications* **13**, 3229 (2022).
 - [10] R. Bhatt and A. Krishna, Topology and many-body localization, *Annals of Physics* **435**, 168438 (2021), special Issue on Localisation 2020.
 - [11] N. Avraham, J. Reiner, A. Kumar-Nayak, N. Morali, R. Batabyal, B. Yan, and H. Beidenkopf, Quasi-particle interference studies of quantum materials, *Advanced Materials* **30**, 1707628 (2018),

- <https://onlinelibrary.wiley.com/doi/pdf/10.1002/adma.201707628> *Phys. Rev. B* **106**, 174406 (2022).
- [12] S.-S. Lee, Recent developments in non-fermi liquid theory, *Annual Review of Condensed Matter Physics* **9**, 227 (2018), <https://doi.org/10.1146/annurev-conmatphys-031016-025531>.
- [13] E. F. Shender and P. C. W. Holdsworth, Order by disorder and topology in frustrated magnetic systems, in *Fluctuations and Order: The New Synthesis*, edited by M. Millonas (Springer US, New York, NY, 1996) pp. 259–279.
- [14] D. Bergman, J. Alicea, E. Gull, S. Trebst, and L. Balents, Order-by-disorder and spiral spin-liquid in frustrated diamond-lattice antiferromagnets, *Nature Physics* **3**, 487 (2007).
- [15] M. Brando, D. Belitz, F. M. Grosche, and T. R. Kirkpatrick, Metallic quantum ferromagnets, *Rev. Mod. Phys.* **88**, 025006 (2016).
- [16] P. Anderson, Resonating valence bonds: A new kind of insulator?, *Materials Research Bulletin* **8**, 153 (1973).
- [17] L. Balents, Spin liquids in frustrated magnets, *Nature* **464**, 199 (2010).
- [18] C. Broholm, R. J. Cava, S. A. Kivelson, D. G. Nocera, M. R. Norman, and T. Senthil, Quantum spin liquids, *Science* **367**, eaay0668 (2020), <https://www.science.org/doi/pdf/10.1126/science.aay0668>.
- [19] K. Binder and A. P. Young, Spin glasses: Experimental facts, theoretical concepts, and open questions, *Rev. Mod. Phys.* **58**, 801 (1986).
- [20] S. Kundu, A. Shahee, A. Chakraborty, K. M. Ranjith, B. Koo, J. Sichelschmidt, M. T. F. Telling, P. K. Biswas, M. Baenitz, I. Dasgupta, S. Pujari, and A. V. Mahajan, Gapless quantum spin liquid in the triangular system $\text{Sr}_3\text{CuSb}_2\text{O}_9$, *Phys. Rev. Lett.* **125**, 267202 (2020).
- [21] I. Kimchi, J. P. Sheckelton, T. M. McQueen, and P. A. Lee, Scaling and data collapse from local moments in frustrated disordered quantum spin systems, *Nature Communications* **9**, 4367 (2018).
- [22] C. Dasgupta and S.-k. Ma, Low-temperature properties of the random heisenberg antiferromagnetic chain, *Phys. Rev. B* **22**, 1305 (1980).
- [23] M. P. Sarachik, A. Roy, M. Turner, M. Levy, D. He, L. L. Isaacs, and R. N. Bhatt, Scaling behavior of the magnetization of insulating Si:P , *Phys. Rev. B* **34**, 387 (1986).
- [24] A. Roy, M. Sarachik, and R. Bhatt, Scaling behavior of the magnetization of Si:B , *Solid State Communications* **60**, 513 (1986).
- [25] R. N. Bhatt and P. A. Lee, Scaling studies of highly disordered spin- $\frac{1}{2}$ antiferromagnetic systems, *Phys. Rev. Lett.* **48**, 344 (1982).
- [26] M. A. Paalanen, J. E. Graebner, R. N. Bhatt, and S. Sachdev, Thermodynamic behavior near a metal-insulator transition, *Phys. Rev. Lett.* **61**, 597 (1988).
- [27] S. Bogdanovich, P. Dai, M. P. Sarachik, and V. Dobrosavljevic, Universal scaling of the magnetoconductance of metallic Si:B , *Phys. Rev. Lett.* **74**, 2543 (1995).
- [28] A. Roy and M. P. Sarachik, Susceptibility of Si:P across the metal-insulator transition. ii. evidence for local moments in the metallic phase, *Phys. Rev. B* **37**, 5531 (1988).
- [29] H. Murayama, T. Tominaga, T. Asaba, A. d. O. Silva, Y. Sato, H. Suzuki, Y. Ukai, S. Suetsugu, Y. Kasahara, R. Okuma, I. Kimchi, and Y. Matsuda, Universal scaling of specific heat in the $s = \frac{1}{2}$ quantum kagome antiferromagnet herbertsmithite, *Phys. Rev. B* **106**, 174406 (2022).
- [30] S. Kundu, A. Hossain, P. K. S., R. Das, M. Baenitz, P. J. Baker, J.-C. Orain, D. C. Joshi, R. Mathieu, P. Mahadevan, S. Pujari, S. Bhattacharjee, A. V. Mahajan, and D. D. Sarma, Signatures of a spin- $\frac{1}{2}$ cooperative paramagnet in the diluted triangular lattice of Y_2CuTiO_6 , *Phys. Rev. Lett.* **125**, 117206 (2020).
- [31] H. Murayama, Y. Sato, T. Taniguchi, R. Kurihara, X. Z. Xing, W. Huang, S. Kasahara, Y. Kasahara, I. Kimchi, M. Yoshida, Y. Iwasa, Y. Mizukami, T. Shibauchi, M. Konczykowski, and Y. Matsuda, Effect of quenched disorder on the quantum spin liquid state of the triangular-lattice antiferromagnet $1t - \text{TaS}_2$, *Phys. Rev. Res.* **2**, 013099 (2020).
- [32] P. A. Volkov, C.-J. Won, D. I. Gorbunov, J. Kim, M. Ye, H.-S. Kim, J. H. Pixley, S.-W. Cheong, and G. Blumberg, Random singlet state in $\text{Ba}_5\text{CuIr}_3\text{O}_{12}$ single crystals, *Phys. Rev. B* **101**, 020406 (2020).
- [33] K. Uematsu and H. Kawamura, Randomness-induced quantum spin liquid behavior in the $s = 1/2$ random-bond heisenberg antiferromagnet on the pyrochlore lattice, *Phys. Rev. Lett.* **123**, 087201 (2019).
- [34] See the Supplemental Material (see also references [37–42] therein) for further details about sample preparation, experimental conditions, x-ray diffraction, magnetic susceptibility analysis, estimation of lattice heat capacity and analytical theoretical calculations..
- [35] Y. Singh, Y. Tokiwa, J. Dong, and P. Gegenwart, Spin liquid close to a quantum critical point in $\text{Na}_4\text{Ir}_3\text{O}_8$, *Phys. Rev. B* **88**, 220413 (2013).
- [36] T. Dey, M. Majumder, J. C. Orain, A. Senyshyn, M. Prinz-Zwick, S. Bachus, Y. Tokiwa, F. Bert, P. Khuntia, N. Büttgen, A. A. Tsirlin, and P. Gegenwart, Persistent low-temperature spin dynamics in the mixed-valence iridate $\text{Ba}_3\text{InIr}_2\text{O}_9$, *Phys. Rev. B* **96**, 174411 (2017).
- [37] M.-E. Song, D. Maurya, Y. Wang, J. Wang, M.-G. Kang, D. Walker, P. A. Thomas, S. T. Huxtable, R. J. Bodnar, N. Q. Vinh, and S. Priya, Phase transitions and phonon mode dynamics of $\text{Ba}(\text{Cu}_1/3\text{Nb}_2/3)\text{O}_3$ and $\text{Sr}(\text{Cu}_1/3\text{Nb}_2/3)\text{O}_3$ for understanding thermoelectric response, *ACS Applied Energy Materials* **3**, 3939 (2020).
- [38] H. D. Zhou, E. S. Choi, G. Li, L. Balicas, C. R. Wiebe, Y. Qiu, J. R. D. Copley, and J. S. Gardner, Spin liquid state in the $s = 1/2$ triangular lattice $\text{Ba}_3\text{CuSb}_2\text{O}_9$, *Phys. Rev. Lett.* **106**, 147204 (2011).
- [39] T. Dey, A. V. Mahajan, P. Khuntia, M. Baenitz, B. Koteswararao, and F. C. Chou, Spin-liquid behavior in $J_{\text{eff}} = \frac{1}{2}$ triangular lattice compound $\text{Ba}_3\text{IrTi}_2\text{O}_9$, *Phys. Rev. B* **86**, 140405 (2012).
- [40] C. Y. Jiang, Y. X. Yang, Y. X. Gao, Z. T. Wan, Z. H. Zhu, T. Shiroka, C. S. Chen, Q. Wu, X. Li, J. C. Jiao, K. W. Chen, Y. Bao, Z. M. Tian, and L. Shu, Spin excitations in the quantum dipolar magnet $\text{Yb}(\text{BaBO}_3)_3$, *Phys. Rev. B* **106**, 014409 (2022).
- [41] K. Somesh, S. S. Islam, S. Mohanty, G. Simutis, Z. Guguchia, C. Wang, J. Sichelschmidt, M. Baenitz, and R. Nath, Absence of magnetic order and emergence of unconventional fluctuations in the $J_{\text{eff}} = \frac{1}{2}$ triangular-lattice antiferromagnet YbBO_3 , *Phys. Rev. B* **107**, 064421 (2023).
- [42] S. Mohanty, S. S. Islam, N. Winterhalter-Stocker, A. Jesche, G. Simutis, C. Wang, Z. Guguchia, J. Sichelschmidt, M. Baenitz, A. A. Tsirlin, P. Gegen-

wart, and R. Nath, Disordered ground state in the spin-

orbit coupled $J_{\text{eff}} = \frac{1}{2}$ distorted honeycomb magnet
biybg₅, [Phys. Rev. B **108**, 134408 \(2023\)](#)